Available online at www.sciencedirect.com
ScienceDirect
Nuclear Physics B 821 (2009) 48–64
NUCLEAR PHYSICS B
www.elsevier.com/locate/nuclphysb

Exploring the universal extra dimension at the LHC

Gautam Bhattacharyya [a,*], Anindya Datta [b], Swarup Kumar Majee [c], Amitava Raychaudhuri [d,b]

[a] *Saha Institute of Nuclear Physics, 1/AF Bidhan Nagar, Kolkata 700064, India*
[b] *Department of Physics, University of Calcutta, 92 A.P.C. Road, Kolkata 700009, India*
[c] *Center for Particle Physics and Phenomenology (CP3), Université Catholique de Louvain, Chemin du Cyclotron 2, B-1348 Louvain-la-Neuve, Belgium*
[d] *Harish-Chandra Research Institute, Chhatnag Road, Jhunsi, Allahabad 211019, India*

Received 23 April 2009; accepted 10 June 2009

Available online 13 June 2009

Abstract

Besides supersymmetry, the other prime candidate of physics beyond the Standard Model (SM), crying out for verification at the CERN Large Hadron Collider (LHC), is extra-dimension. To hunt for effects of Kaluza–Klein (KK) excitations of known fermions and bosons is very much in the agenda of the LHC. These KK states arise when the SM particles penetrate in the extra space-like dimension(s). In this paper, we consider a 5d scenario, called 'Universal Extra Dimension', where the extra space coordinate, compactified on an orbifold S^1/Z_2, is accessed by *all* the particles. The KK number (n) is conserved at all tree level vertices. This entails the production of KK states in pairs and renders the lightest KK particle stable, which leaves the detector carrying away missing energy. The splitting between different KK flavors is controlled by the zero mode masses and the bulk- and brane-induced one-loop radiative corrections. We concentrate on the production of an $n = 1$ KK electroweak gauge boson in association with an $n = 1$ KK quark. This leads to a signal consisting of *only one* jet, one or more leptons and missing p_T. For definiteness we usually choose the inverse radius of compactification to be $R^{-1} = 500$ GeV, which sets the scale of the lowest lying KK states. We show on a case-by-case basis (depending on the number of leptons in the final state) that with 10 fb^{-1} integrated luminosity at the LHC with $\sqrt{s} = 14$ TeV this signal can be detected over the SM background by imposing appropriate kinematic cuts. We record some of the expectations for a possible intermediate LHC run at $\sqrt{s} = 10$ TeV and also exhibit the integrated luminosity required to obtain a 5σ signal as a function of R^{-1}.

* Corresponding author.
E-mail address: gautam.bhattacharyya@saha.ac.in (G. Bhattacharyya).

0550-3213/$ – see front matter
doi:10.1016/j.nuclphysb.2009.06.010

PACS: 12.60.-i; 04.50.Cd; 13.85.-t

Keywords: Universal extra dimension; Kaluza–Klein particles; LHC

1. Introduction

Probing the origin of electroweak symmetry breaking (EWSB) constitutes the prime mandate of the CERN LHC, a proton–proton collider set to operate at $\sqrt{s} = 14$ TeV. Unprecedented efforts are going to be invested not only for the search for the SM Higgs boson, but also for exploring other avenues which can successfully trigger EWSB. Among them, supersymmetry and extra-dimension stand out as two potential rulers of the tera-electron-volt regime, which is the region of energies and distances to be unplugged at the LHC. Although string models are intrinsically extra-dimensional, the phenomenological implications of extra dimensions were first studied in the context of a scenario [1] in which gravity propagates in a compact and flat millimeter size ($1\ \text{mm}^{-1} = 10^{-3}$ eV) extra-dimensional bulk with the SM particles confined to a 4d brane. The fundamental Planck scale is then brought down to around a TeV making it accessible to the collider experiments. Subsequently, the concept of a 'fat-brane' was introduced [2] in which the SM particles are not strictly confined to a point in the extra dimension but travel within the size of the brane, which may be considered as a bulk of much smaller compactified dimension. In the present analysis, we attempt to extract possible signals of such fat-brane scenarios at the LHC, when the size of the brane is order TeV.

Studies based on a scenario in which only the SM gauge bosons access the bulk while the fermions are confined to a 4d brane [3] reveal that R^{-1} cannot be below 1–2 TeV. The bound originates from several considerations: Drell–Yan processes in hadron colliders [4], $e^+e^- \to \mu^+\mu^-$ at LEP2 [5], electroweak precision tests [6], etc. Because the fermions are treated differently from the bosons, such scenarios are called nonuniversal extra-dimensional models (NUED). On the other hand, in what is called the universal extra-dimensional model (UED) [7], where *all* the SM particles access the extra dimension, the constraint is not that tight. UED is relatively easy to motivate compared to NUED as one does not have to selectively confine the SM fields in a 4d brane. One crucial difference between UED and NUED is that the quantized momentum along the extra space direction, conventionally labeled by the KK number, is conserved for the former but not for the latter. Thus while in NUED the KK states mediate processes such as $e^+e^- \to f\bar{f}$ at tree level incurring very strong experimental constraints, in UED the KK states appear only in loops resulting in milder bounds. Moreover, one-loop processes in NUED are ultraviolet-divergent while in UED they are finite [8]. Analysis of constraints on UED from $g-2$ of the muon [9], flavor changing neutral currents [10–12], $Z \to b\bar{b}$ decay [13], the ρ parameter [7,14], hadron collider studies [15], all reveal that $R^{-1} \gtrsim 300$ GeV. Consideration of $b \to s\gamma$, however, implies a somewhat tighter bound ($R^{-1} \gtrsim 600$ GeV [16]). In fact, UED should be perceived more as a bare structure with a basic minimum on top of which further details can be attributed to build separate models for addressing different issues. Several implications of UED have already been investigated from the perspective of high energy experiments, phenomenology, string theory, cosmology, and astrophysics. To name a few, such TeV scale flat extra-dimensional scenarios can provide a cosmologically viable dark matter candidate [17], address the issue of fermion

mass hierarchy from a different angle [18],[1] interpret the Higgs as a quark composite leading to a successful EWSB without the necessity of a fundamental Yukawa interaction [20], and lower the unification scale down to a few tens of a TeV [21–23]. In the supersymmetric context, a new mechanism of supersymmetry breaking related to compactification has been advanced [2], which at the same time ameliorates the hierarchy problem that an otherwise non-supersymmetric set-up suffers from. Furthermore, the upper limit of the lightest supersymmetric neutral Higgs has been shown to be relaxed [24]. Our present analysis is, however, based on a non-supersymmetric set-up.

Let us now get into the specifics of UED. There is a single flat extra dimension (y), compactified on an S^1/Z_2 orbifold, and accessed by all the SM particles [7]. From a 4d point of view, each field will have an infinite tower of KK modes, the zero modes being identified as the SM states. The orbifolding is essential to ensure that fermion zero modes have a chiral representation. But it has other consequences too. *First*, the physical region along the extra direction y is now smaller $[0, \pi R]$ than the periodicity $[0, 2\pi R]$, so the KK number (n) is no longer conserved. What remains actually conserved is the even-ness and odd-ness of the KK states, ensured through the conservation of KK parity, defined by $(-1)^n$. *Secondly*, Lorentz invariance is also lost due to compactification, and as a result the KK masses receive bulk and orbifold-induced radiative corrections [25–28]. The bulk corrections are finite and nonzero only for bosons. The orbifold corrections, which vary logarithmically with the cutoff, depend on group theoretic invariants, as well as Yukawa and quartic scalar couplings of the gauge and matter KK fields and hence are flavor-dependent. This induces a mass splitting among the different flavors of the same KK level, further to what has already been caused by the different zero mode masses. Typically, if $R^{-1} = 500$ GeV, the lightest among the $n = 1$ KK states turns out to be γ^1 weighing slightly above 500 GeV, just above lie the KK leptons and weak bosons in the region of 500–550 GeV, further up are the KK quarks near 600 GeV, and at the peak the KK gluon (the heaviest) hovers around 650 GeV.

Possibility of detection of UED KK states has already been studied in the context of hadron colliders [29]. Two distinct scenarios have been investigated: (i) the KK states are stable within the size of the detector (the radiative origin of splitting was not considered here); (ii) although γ^1 is the lightest KK state (considering the radiative splitting), the KK number violating interaction at the brane-bulk interface makes it decay within the detector to a photon and a graviton (missing particle). In either of the two options, a lower limit of 350–400 GeV was set on the mass of KK quarks and gluon from Tevatron Run-I data, while the Run-II data improved the limit to 500 GeV. It was anticipated that LHC would either discover such states or at least push the limit to about 3 TeV. Another approach was followed in [30], where the KK states could decay into zero mode states by KK number violation, and a reach of 3 TeV for KK quarks and gluon was envisaged with 100^{-1} fb luminosity at the LHC.

Although the broad framework within which we work in this paper is the same UED as pursued in [29] and [30], we differ in some details of the model. As a result, our final states are different from theirs, and hence a comparison of these analyses is not straightforward. Throughout, we strictly adhere to the conservation of the KK number at all *tree level* vertices and KK

[1] If generation universality is assumed in the localization of different fermions, a global fit to electroweak observables yields $R^{-1} \gtrsim$ (2–5) TeV. When this universality is sacrificed, e.g. in an attempt to address the fermion hierarchy problem [18], KK gauge bosons pick up tree level couplings with different generation of fermions leading to large flavor-changing neutral currents and CP violation. Such scenarios cease to be of any relevance at the TeV scale, as considerations of Δm_K, ϵ_K and ϵ'_K push the lower limit on R^{-1} to around 5000 TeV [19].

parity to all order. This means that our γ^1 is stable. Then, once the KK states are produced, the decay patterns and branching ratios are decided depending on the relative amount of radiative splittings among the different $n = 1$ KK modes. The end products are (at least) two γ^1, carrying away missing energy, plus the SM zero modes. Note, $\sigma(Q^1\bar{Q}^1) > \sigma(Q^1V^1) > \sigma(V^1V^1)$, where Q^1 and V^1 stand for generic KK quark and KK electroweak gauge boson, respectively. When both particles at the production vertex are KK quarks/gluons, although the cross section is very high, nonetheless, the final states following their decays contain more than one jet making way to very large SM backgrounds. On the other hand, if both parent KK particles are color neutral, the final states are hadronically quiet with significantly reduced SM background but the overall signal production cross section turns out to be quite low. Therefore, we focus on the production of the mixed combination, namely Q^1V^1, which is optimally balanced from the signal and background perspectives. Following the decay chain, we are led to the following final state configuration: *only one* jet, n_l number of leptons (n_l could be zero to four), and two γ^1 (missing energy). This is a path so far not travelled in the hunt for KK states in a hadronic machine. As we will see, for $R^{-1} \sim 500$ GeV this signal can be comprehensively deciphered from the SM background with modest integrated luminosities by designing suitable kinematic cuts.

It is important to mention at this stage that although UED and supersymmetry are structurally very different theories, ironically, their collider signatures tantalizingly mimic each other [31]. Possible methods of distinction of UED signals from supersymmetry, mainly based on spin studies, have been carried out both in the context of the LHC [32,33] and the (future) linear collider [34]. These discriminations require accurate theoretical tools with advanced Monte Carlos offering high sensitivity to small deviation. In this work, we do not intend to entertain such multiple possibilities of what might lie at this hazy domain across the new frontier. Rather, we consider UED as the only new physics and intend to isolate its signals from possible SM background. Mainly because of this working hypothesis, a parton-level Monte Carlo that we employ is good enough for our simulation. We observe that following our strategy KK states can be spotted at the LHC for R^{-1} all the way up to 700–800 GeV for an integrated luminosity of 100–300 fb^{-1}.

The paper is organised as follows. In the next section, we briefly introduce UED, write down the mode expansions of different fields, and give an estimation of the radiative corrections to different KK masses. In the subsequent section, we discuss the production of a first level KK quark in association with the KK gauge bosons and their different decay chains. Then, we discuss the relative efficiency of background elimination by looking for signals with different number of leptons in the final state. In the last section, we summarize and conclude.

2. Universal extra dimension

2.1. Mode expansions

The extra coordinate y is compactified on a circle of radius R with a Z_2 orbifolding identifying y with $-y$. The orbifolding is essential for generating zero mode *chiral* fermions. After the y-dependence is integrated out, the 4d Lagrangian contains the zero mode and the KK modes of different fields. Let us now take a look at the KK mode expansions of these fields. Since Z_2 is a symmetry of the theory, each 5d field must be either even or odd under this discrete parity. The KK expansions are given by

$$A_\mu(x, y) = \frac{\sqrt{2}}{\sqrt{2\pi R}} A_\mu^0(x) + \frac{2}{\sqrt{2\pi R}} \sum_{n=1}^{\infty} A_\mu^n(x) \cos\frac{ny}{R},$$

$$
\begin{aligned}
A_5(x,y) &= \frac{2}{\sqrt{2\pi R}}\sum_{n=1}^{\infty} A_5^n(x)\sin\frac{ny}{R},\\
\phi(x,y) &= \frac{\sqrt{2}}{\sqrt{2\pi R}}\phi^0(x) + \frac{2}{\sqrt{2\pi R}}\sum_{n=1}^{\infty}\phi^n(x)\cos\frac{ny}{R},\\
\mathcal{Q}_i(x,y) &= \frac{\sqrt{2}}{\sqrt{2\pi R}}\left[\begin{pmatrix} u_i \\ d_i\end{pmatrix}_L(x) + \sqrt{2}\sum_{n=1}^{\infty}\left[\mathcal{Q}_{iL}^n(x)\cos\frac{ny}{R} + \mathcal{Q}_{iR}^n(x)\sin\frac{ny}{R}\right]\right],\\
\mathcal{U}_i(x,y) &= \frac{\sqrt{2}}{\sqrt{2\pi R}}\left[u_{iR}(x) + \sqrt{2}\sum_{n=1}^{\infty}\left[\mathcal{U}_{iR}^n(x)\cos\frac{ny}{R} + \mathcal{U}_{iL}^n(x)\sin\frac{ny}{R}\right]\right],\\
\mathcal{D}_i(x,y) &= \frac{\sqrt{2}}{\sqrt{2\pi R}}\left[d_{iR}(x) + \sqrt{2}\sum_{n=1}^{\infty}\left[\mathcal{D}_{iR}^n(x)\cos\frac{ny}{R} + \mathcal{D}_{iL}^n(x)\sin\frac{ny}{R}\right]\right],
\end{aligned}
\tag{1}
$$

where $i = 1, 2, 3$ are generation indices. The complex scalar field $\phi(x, y)$ and the gauge boson $A_\mu(x, y)$ are Z_2-even fields, and their zero modes are identified with the SM scalar and gauge boson, respectively. The field $A_5(x, y)$ is a real scalar transforming in the adjoint representation of the gauge group, and it does not have any zero mode. The fields $\mathcal{Q}$, $\mathcal{U}$, and $\mathcal{D}$ describe the 5d quark doublet and singlet states, respectively, whose zero modes correspond to the chiral SM quark states. The mode expansions of the doublet and singlet leptons can be written *mutatis mutandis*.

2.2. Radiative corrections to the KK masses

At a given n, the KK mass is given by $\sqrt{m_0^2 + n^2/R^2}$. So, *modulo* the zero mode masses, the KK states are degenerate. But this is only a tree level result. Radiative corrections lift this degeneracy [25–28]. To provide intuition, let us consider the kinetic term of a scalar field as [25] $L_{\rm kin} = Z\partial_\mu\phi\partial^\mu\phi - Z_5\partial_5\phi\partial^5\phi$ ($\mu = 0, 1, 2, 3$), where Z and Z_5 are renormalization constants. Recall that tree level KK masses originate from the kinetic term in the y-direction. If $Z = Z_5$, there is no correction to those masses. But this equality follows from Lorentz invariance. When a direction is compactified, Lorentz invariance breaks down. Then $Z \neq Z_5$, leading to $\Delta m_n \propto (Z - Z_5)$. More specifically, there are two kinds of radiative corrections.

Bulk correction. These corrections are finite and nonzero only for bosons. They arise whenever the internal loops wind around the compactified direction. These corrections, for a given field, are the same for any KK mode. For a KK boson mass $m_n(B)$, these corrections are given by

$$
\delta m_n^2(B) = \kappa\frac{\zeta(3)}{16\pi^4}\left(\frac{1}{R}\right)^2,
\tag{2}
$$

where κ is a collective representation of group invariants, being equal to $-39g_1^2/2$, $-5g_2^2/2$ and $-3g_3^2/2$ for B^n, W^n and g^n, respectively. Clearly, for $R \to \infty$, one recovers the original Lorentz invariance and the correction vanishes.

Orbifold correction. Orbifolding additionally breaks translational invariance in the y-direction. The corrections to the KK masses arising from interactions localized at the fixed points are logarithmically divergent. The corrections can be thought of as counterterms whose

Table 1
Radiatively corrected first KK-mode masses (all in GeV) for $R^{-1} = 500$ GeV and $\Lambda R = 20$. The values of a, b, c, introduced in Eq. (3), are displayed. While assigning b and c for γ^1 and Z^1, we used $\theta_W^1 \to 0$.

States	Q^1	u^1	d^1	L^1	e^1	g^1	$W^{\pm 1}$	Z^1	γ^1
Mass	598.7	587.3	585.5	515	505.5	642.3	536	542.1	501.0
a	3	3	3	0	0	23/2	0	0	0
b	27/16	0	0	27/16	0	0	15/2	15/2	0
c	1/16	1	1/4	9/16	9/4	0	0	0	−1/6

finite parts are unknown. We just follow a predictive hypothesis that these corrections vanish at the cutoff scale Λ. The amount of this correction to a generic KK fermion mass $m_n(f)$, or a KK gauge boson mass $m_n(B)$, is given by

$$\frac{\delta m_n(f)}{m_n(f)}\left(\frac{\delta m_n^2(B)}{m_n^2(B)}\right) = \left(a\frac{g_3^2}{16\pi^2} + b\frac{g_2^2}{16\pi^2} + c\frac{g_1^2}{16\pi^2}\right)\ln\frac{\Lambda^2}{\mu^2}, \tag{3}$$

where a, b and c for different KK states are listed in Table 1. As it turns out, the orbifold corrections are numerically more significant than the bulk corrections.

The mass squared matrix of the neutral KK gauge boson sector in the B_n, W_n^3 basis is given by

$$\begin{pmatrix} \frac{n^2}{R^2} + \hat{\delta} m_{B_n}^2 + \frac{1}{4}g_1^2 v^2 & \frac{1}{4}g_1 g_2 v^2 \\ \frac{1}{4}g_1 g_2 v^2 & \frac{n^2}{R^2} + \hat{\delta} m_{W_n}^2 + \frac{1}{4}g_2^2 v^2 \end{pmatrix}, \tag{4}$$

where $\hat{\delta}$ represents the sum of bulk and orbifold radiative corrections. The KK photon and Z boson states are obtained by diagonalizing the above matrix. Note, the value of the weak mixing angle for the KK states is sizably altered from the zero mode value ($\sin^2\theta_W \simeq 0.23$) due to a difference in size of those $\hat{\delta}$-terms in the mass squared matrix in Eq. (4). The modified value is different for different choices of n and R. For $n = 1$ and $R^{-1} = 500$ GeV, it turns out that $\sin^2\theta_W^1 \sim 0.01$, i.e., γ^1 and Z^1 are primarily B^1 and W_3^1, respectively.

In Table 1, we present the masses for different $n = 1$ KK excitations to assess the extent to which the radiative corrections lift the degeneracy. For illustration, we take $R^{-1} = 500$ GeV and $\Lambda R = 20$ (a rough justification for this choice is that the gauge couplings, following a power law renormalization group running, tend to unify after more or less $\Lambda R = 20$–25 KK resonances are excited).

3. Productions and decay of the first KK-mode

As noted in the previous section, if R^{-1} is not too large, the first KK-excitations of the Standard Model particles are in the right mass range for pair-production at the LHC. We consider the parton-level process[2] $qg \to \bar{Q}V^1$ for which the matrix element square is:

$$\left|\mathcal{M}\{qg \to \bar{Q}V^1\}\right|^2 = \frac{\pi\alpha_s(\hat{s})(a_L^2 + a_R^2)}{6}\left[\frac{\{-2\hat{s}\hat{t} + 2\hat{s}m_{\bar{Q}}^2\}}{\hat{s}^2}\right.$$

[2] Here $\bar{Q}$ stands for the SU(2) doublet (Q^1) as well as the singlet ($q^1 \equiv u^1, d^1$) KK excited quarks.

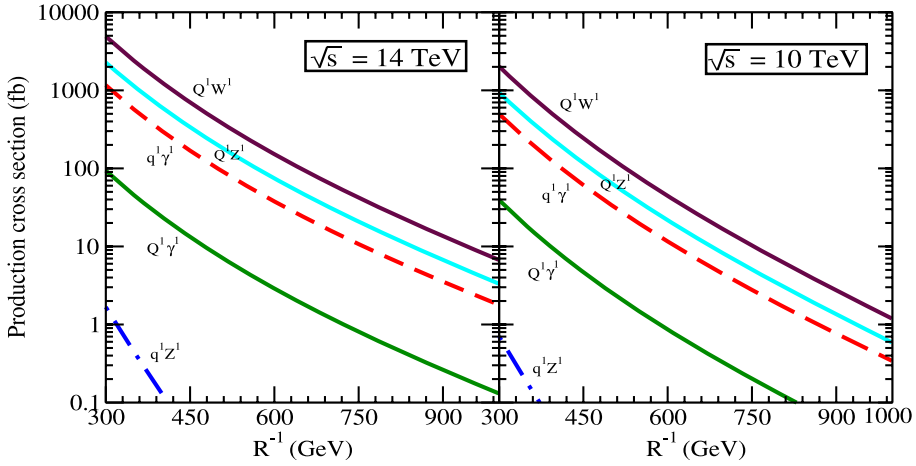

Fig. 1. Cross sections for the associated production of the lightest KK electroweak gauge bosons with the lightest KK quarks. Solid (broken) lines correspond to SU(2) doublet quarks Q^1 (SU(2) singlet quarks q^1). Note that the W^1 cannot be produced with a q^1.

Table 2
The couplings a_L and a_R – involving an excited gauge boson, an excited quark, and an ordinary quark – used in Eq. (5). Note that KK-parity conservation requires a_R (a_L) to vanish for Q (q) in all cases. The couplings of the excited leptons (L^1, l^1) to the excited gauge bosons follow a similar pattern and can be easily read off from this table.

Excited quark →	SU(2) doublet (Q)		SU(2) singlet (q)	
Excited boson ↓	a_R	a_L	a_R	a_L
W^1	0	$\frac{g}{\sqrt{2}}$	0	0
Z^1	0	$\frac{g}{2\cos\theta_W^1}(T_3 - e_Q \sin^2\theta_W^1)$	$-\frac{g}{2\cos\theta_W^1}(e_q \sin^2\theta_W^1)$	0
γ^1	0	$\frac{e_Q}{\cos\theta_W}\cos\theta_W^1$	$\frac{e_q}{\cos\theta_W}\cos\theta_W^1$	0

$$+\frac{\{-2\hat{s}\hat{t}-4\hat{t}m_{\bar{Q}}^2+2\hat{s}m_{\bar{Q}}^2+4m_{V^1}^2m_{\bar{Q}}^2\}}{(\hat{t}-m_{\bar{Q}}^2)^2}$$
$$+\frac{2\{-2\hat{t}m_{\bar{Q}}^2+2(\hat{s}+\hat{t})m_{V^1}^2+2m_{V^1}^2m_{\bar{Q}}^2-2m_{V^1}^4\}}{\hat{s}(\hat{t}-m_{\bar{Q}}^2)}\Bigg], \tag{5}$$

where $\hat{s}$ and $\hat{t}$ are the (parton-level) Mandelstam variables. The couplings a_L and a_R are fixed by the final state particles and are summarized in Table 2. They depend on the weak mixing angle of the excited bosons, θ_W^1, which is a function of R^{-1} and is considerably smaller than θ_W. The KK-excitations of quarks and leptons are vector-like fermions, so, unlike for the SM fermions, the couplings listed for 'singlet' or 'doublet' quarks have both chiral counterparts.

The cross sections for the various channels at the LHC with $\sqrt{s} = 14$ TeV and 10 TeV (evaluated using CTEQ6 parton distributions (leading order parametrization) [35] with $Q^2 = \hat{s}$)[3] are shown as a function of R^{-1} in Fig. 1. The cross sections fall rapidly with R^{-1} and vary over

[3] We have performed two independent checks to assess the QCD uncertainties. The MRST parton distribution function, we have checked, yields cross sections which at the leading order are within 10% of the CTEQ6L1 results. We also varied

Table 3
The zero-mode quarks or leptons produced from the decays of Z^1, $(W^1)^\pm$, q^1, and Q^1. In addition, a γ^1 is also produced in all decays.

Parent particle	Z^1	$(W^1)^\pm$	q^1	Q^1
Decay products	$(L^\pm + L^\mp)$ or $(\nu\nu)$	$L^\pm + \nu$	q	$Q + (L^\pm + L^\mp)$ or $(\nu\nu)$ or $Q' + (L^\pm + \nu)$

several orders of magnitude, $q^1 Z^1$ having the smallest cross section and $Q^1 W^1$ the largest (in pb order for $R^{-1} \sim 500$ GeV).[4]

We next turn to the expected final state event topologies. These can be ascertained from the decay characteristics of the excited quarks and gauge bosons. The possible decay channels and branching ratios have been listed in [31]. For the discussions below, it is worth noting that $\sin^2\theta_W^1 \ll \sin^2\theta_W$.

- Excited γ (γ^1): γ^1 is the lightest Kaluza–Klein particle (LKP). This particle is uncharged and stable due to KK-parity conservation. When produced, it escapes detection.
- Excited Z (Z^1): The Z^1 being lighter than the excited quark states cannot decay to them. Nor is the decay to a Z and γ^1 kinematically allowed. So, a Z^1 will decay to the final states[5] $(L^1)^\pm L^\mp$ and $\nu^1\nu$ with equal branching ratios.[6] In the former case there is the subsequent decay $L^1 \to L\gamma^1$ of which only the lepton is observable and the γ^1 remains undetected. This leads to a final Z^1 signal consisting of two (oppositely) charged leptons of the same flavor and missing p_T.
- Excited W (W^1): Kinematics does not permit the $(W^1)^\pm$ to decay hadronically or to $W^\pm\gamma^1$. Consequently, it decays to either $L^\pm\nu^1$ or to $(L^1)^\pm\nu$ with equal branching ratios. The final decay products are therefore $L^\pm\nu\gamma^1$ of which only the charged lepton is observable.
- SU(2) singlet excited quarks (q^1): The SU(2) singlet excited quark decays predominantly to a zero-mode quark and a γ^1. The coupling to Z^1 is suppressed by $\sin^2\theta_W^1$.
- SU(2) doublet excited quarks (Q^1): These can decay to a zero-mode quark doublet Q and any of the excited gauge bosons W^1, Z^1, γ^1. However, the dominant decay modes turn out to be [31] the first two modes with a 2 : 1 ratio.

The zero-mode quarks and leptons produced from the decay of different excited gauge bosons and quarks are listed in Table 3. In addition to the particles shown, there is always a γ^1 in the final state carrying away missing p_T. As a consequence, $(Q^1V^1)/(q^1V^1)$ production results in a final state containing 1-jet + n_l leptons + missing p_T. Depending on the decay modes of the excited quark and V^1, the number of leptons, n_l, can be 0 to 4. In the following, we will classify the signal according to the number of detected leptons and compare it with the SM background.

In our analysis we include contributions from both electron and muon final states. Tau-leptons will also be produced at essentially the same rates. Conservatively, we have not included the

the scale Q^2, which we kept common for both parton density and α_S, from $2\hat{s}$ to $0.5\hat{s}$, and observed that the leading order cross sections alter by about (7–8)% around the values quoted for $Q^2 = \hat{s}$.

[4] Our cross sections are in almost complete agreement with the ones obtained using MADGRAPH [36] and FEYNRULES [37] (more precisely, FR-MUED).

[5] Recall that L (l) represents the SU(2) doublet (singlet) charged lepton state.

[6] The decay $Z^1 \to (l^1)^\pm l^\mp$ is suppressed by $\sin^2\theta_W^1$.

Table 4
Cross section (in fb) for multilepton channels of the signal (for $R^{-1} = 500$ GeV and 1 TeV) and SM background at the LHC with $\sqrt{s} = 14$ TeV after the basic cuts. The two-lepton number corresponds to e^+e^- or $\mu^+\mu^-$.

Channel	$0l$	$1l$	$2l$	$3l$	$4l$
Signal (500 GeV)	106.4	17.92	29.58	9.39	1.01
Signal (1 TeV)	2.02	0.35	0.606	0.210	0.025
Background	4.7×10^5	1.3×10^6	8.6×10^4	1183.21	0.13

states arising from their purely leptonic decays (branching ratio ~ 0.17 to electrons or muons) which would produce e^+e^-, $\mu^+\mu^-$, and $e^\pm\mu^\mp$ events in the ratio $1:1:2$.

4. Multilepton signals and backgrounds

In this section, one by one we consider the different multilepton final states which may arise from $(Q^1V^1)/(q^1V^1)$ production. Table 3 will be of use for the discussions below. As stressed earlier, in addition to the leptons, there is always one hadronic jet and missing transverse momentum, $\not{p}_T$, in the signal.

Basic cuts. For the signal and the background a minimal cut of $p_T{}^{\rm jet} > 20$ GeV has been applied while leptons are required to satisfy $p_T > 5$ GeV. A cut of $\not{p}_T > 25$ GeV has also been used. To evade a possible large background from lepton pairs produced by soft photons we require $M_{l_il_j} > 5$ GeV in multilepton events. A rapidity cut of $|\eta| < 2.5$ is applied for leptons and the jet. We call these the 'basic' cuts.

Numerical values of the cross sections after the basic cuts are listed in Table 4 for two different values of R^{-1} along with the backgrounds. We have estimated the SM backgrounds at the partonic level using MADGRAPH. CTEQ6 parton distribution functions are utilised. It is seen that the backgrounds far overwhelm the signals in all cases but for the 4-lepton one. Further kinematic cuts, discussed below, are needed to enhance the signal *vis-à-vis* the background.

4.1. No lepton

This case will result from the production of (i) $q^1\gamma^1$ and (ii) q^1Z^1 followed by an invisible decay ($\nu\nu\gamma^1$) of the Z^1. It is seen from Table 4 that the signal cross section after the basic cuts is rather large compared to the other cases since there is no branching ratio (to lepton) suppression incurred here. This is unfortunately offset by the very huge SM background in this channel. In this work our interest is to use the multilepton final state to reduce the SM background. So, this no-lepton topology is not pursued any further.

4.2. One lepton

This final state can arise from (i) Q^1Z^1 (and $Q^1\gamma^1$) production followed by the decay $Q^1 \to Q'W^1$ and an invisible Z^1 decay, and (ii) Q^1W^1 followed by $Q^1 \to QZ^1$ and an invisible Z^1 decay. Whenever there are multiple modes which can contribute to a signal, we have included all of them together in the analysis.

The SM background to this one-lepton signal comes from W-production in association with a jet, followed by leptonic decay of the W-boson. The rate of the irreducible one-lepton background at LHC energies is large compared to the signal cross section. Application of kinematical

cuts is not sufficient to dig the signal out from this background. Unraveling the one-lepton signal over the SM background could be too challenging.

4.3. Two leptons

Next we consider the two-lepton case. The signal can arise from (i) Q^1W^1 production followed by $Q^1 \to Q'W^1$ and (ii) Q^1Z^1 production followed by the decays: $Q^1 \to QZ^1$ and the invisible decay of one of the two Z^1. Note that mode (i) can lead to $e^\pm\mu^\mp$ final states. We separately consider 'like-flavor', i.e., e^+e^- or $\mu^+\mu^-$, as well as 'unlike-flavor', i.e., $\mu^+e^- + e^+\mu^-$, in the following.

The dominant SM background to this final state will be from $t\bar{t}$ and $b\bar{b}$ production followed by their semileptonic decay. In addition, the electroweak production of $t\bar{b}$, $b\bar{t}$ and their subsequent decay is also of significance. These backgrounds are severely cut down by requiring the monojet to satisfy $p_T^{\rm jet} > 20$ GeV and the other basic cuts.

From top-pair production and semileptonic decays of both, two jets are expected. To mimic the signal, one of these jets must fail the jet-p_T cut while the other must pass. In addition, we demand 'lepton isolation' – that all leptons be isolated from the jet satisfying $\Delta R > 0.7$, where $\Delta R^2 = (\Delta\phi^2 + \Delta\eta^2)$. This and the other basic cuts reduce the cross section to 173.2 (79.84) fb for an LHC run with $\sqrt{s} = 14(10)$ TeV. Further kinematic cuts are necessary, as discussed below, to reduce this background.

The $b\bar{b}$ production followed by semileptonic decays has a large cross section of ~ 100 nb at the LHC. However, the low mass of the b-quark ensures that this background is *totally* removed when the basic cuts are imposed along with lepton isolation.

In spite of their electroweak origin, the $t\bar{b}$, $b\bar{t}$ production rates are substantial. The twin requirements of one jet with $p_T^{\rm jet} > 20$ GeV and a lepton isolation cut of $\Delta R > 0.7$ are found to suffice for eliminating this background. After these cuts, this channel contributes 15.94 (10.92) fb to the background for $\sqrt{s} = 14(10)$ TeV.

The remaining SM background is from W pair production in association with a jet. Z pair (real or virtual) or $Z\gamma^*$ (leptons coming from the γ^* with an invisible Z decay) production in association with a jet also contributes to the SM background. The W pair production channel, which is the more relevant one since the on-shell Z background is small and anyway readily removed, results in e^+e^-, $\mu^+\mu^-$, and $e^\pm\mu^\mp$ events in the ratio $1:1:2$. In these cases, the jet is from either gluon or quark radiation off the initial partons, and consequently, most of the time it emerges close to the beam axis. This will be reflected in the rapidity distribution of the jet. This is in contrast with the signal. The basic cut on ${p_T}^{\rm jet}$ helps enhance the strength of the signal over the SM background.

Here, we focus on the case of $\mu^+\mu^-$ + one jet + missing p_T final states. The results are identical if the $\mu^+\mu^-$ are replaced by e^+e^-. Parallely, we will be remarking on the $\mu^\pm e^\mp$ alternative. For $R^{-1} = 500$ GeV, with the LHC running at $\sqrt{s} = 14$ TeV the signal turns out to be much less than the background in both cases (see Table 5). Naturally, for $\sqrt{s} = 10$ TeV the situation is worse. To enhance the signal *vis-à-vis* the background the following further kinematic cuts are suggested[7]:

(i) ${p_T}^{l_1} < 25$ GeV,

[7] l_1 has lower p_T than l_2.

Table 5
Cross section (in fb) at the LHC of signal and background for the like-flavor $\mu^+\mu^-$ or e^+e^- (unlike-flavor $\mu^+e^- + e^+\mu^-$) dilepton plus one jet and missing p_T channel for $R^{-1} = 500$ GeV.

$\sqrt{s}\ \rightarrow$	14 TeV		10 TeV	
Cut used $\downarrow$	Signal	Background	Signal	Background
Basic cuts	29.58 (43.10)	8.6×10^4 (17.2×10^4)	10.00 (14.60)	4.8×10^4 (9.6×10^4)
Lepton isolation	24.24 (35.24)	218.38 (429.64)	8.28 (12.06)	108.54 (212.78)
${p_T}^{l_1} < 25$ GeV	21.66 (30.88)	78.67 (154.90)	7.52 (10.74)	41.10 (80.70)
${p_T}^{l_2} < 25$ GeV	12.58 (18.00)	9.44 (18.40)	4.53 (6.52)	5.27 (10.22)
$\lvert M_{l_1 l_2} - M_Z \rvert > 10$ GeV	12.52 (17.88)	9.18 (17.98)	4.51 (6.48)	5.17 (10.08)

(ii) ${p_T}^{l_2} < 25$ GeV,
(iii) $|M_{l_1 l_2} - M_Z| > 10$ GeV.

The effect of these cuts on the signal (red solid histogram) and the background (blue dotted histogram) are shown in Fig. 2 and also presented in Table 5.

The two cuts on the lepton p_T are chosen on the following grounds. In UED, the leptons arising from the decays (at any stage of the decay chain) of KK-mode excitations are always accompanied by the LKP or some other KK excitation. The small mass splitting between the KK excitations results in a comparatively soft lepton and their p_T distributions will be peaked around lower values and are spread over a limited range. For the SM background, the energy of the parent particles (Z, W or γ^*), which are much lighter than the KK states, is shared between two particles of negligible mass. As a result, p_T distributions of these leptons, though also peaked at lower values, have a tail extended to higher values compared to the signal. So, by demanding the p_T of the leptons to be bounded from above, one can get rid of much of the background. This is exemplified in the top three rows of Fig. 2.

As is seen from Table 5, for the $\sqrt{s} = 14$ TeV case, through the kinematic cuts the background for like- (unlike-)flavor is reduced from 8.6×10^4 (17.2×10^4) fb to 9.18 (17.98) fb. For a modest integrated luminosity of 10 fb^{-1} the significance[8] ($S/\sqrt{S+B}$) after the basic cuts is 0.32 (0.33), which after the kinematic cuts is enhanced to a healthy 8.50 (9.44).

For the discussion so far we have chosen as a reference value $R^{-1} = 500$ GeV. The integrated luminosities necessary for a 5σ signal after the complete set of kinematic cuts as a function of R^{-1} for $\sqrt{s} = 14$ TeV (left) and 10 TeV (right) are plotted in Fig. 3. Both like-flavor (L) $\mu^+\mu^-$ or e^+e^- (blue dot-dashed) and unlike-flavor (U) $\mu^+e^- + e^+\mu^-$ (red-dashed) cases are shown. It is seen that with an integrated luminosity of 100 fb^{-1} for the like-flavor case one can probe the KK states for R^{-1} upto about 700 (600) GeV for the LHC running with $\sqrt{s} = 14$ (10) TeV while for the unlike-flavor case these limits are 620 (570) GeV.

4.4. Three leptons

We now turn to the three-lepton case. As the number of leptons in the final state increases the signal gains over the background. For the signal, channels with different numbers of leptons follow from alternate decay modes of the produced KK particles and the cross sections differ only

[8] Using the above definition of significance is quite appropriate especially since in some cases we are dealing with very low backgrounds following the imposition of the kinematic cuts.

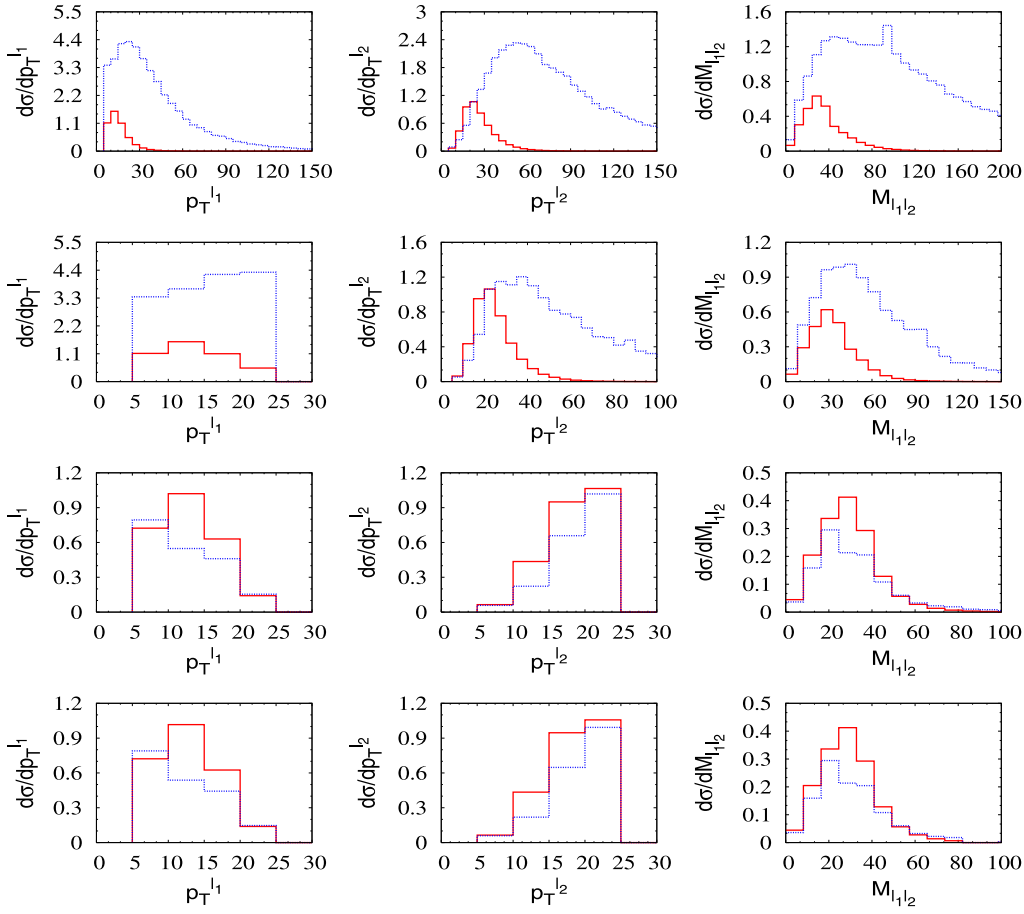

Fig. 2. Two like-flavor leptons ($\mu^+\mu^-$ or e^+e^-) + jet + missing p_T signal (for $R^{-1} = 500$ GeV) and background differential cross sections (in fb/GeV). The solid (red in web version) histograms are for the signal and the dotted (blue in web version) ones are for the background. The successive rows reflect the impact of kinematic cuts shown in Table 5. Lepton isolation cut has already been imposed on the top row.

to the extent of the corresponding branching ratios. On the other hand, a background channel with more leptons usually corresponds to a higher order electroweak process with its concomitant perturbative suppression. Alternatively, it involves a Z-boson decay which can be readily removed by an invariant mass cut. This will be brought out in the three- and four-lepton channels to which we now turn.

The three-lepton final state is realised through (i) Q^1W^1 production followed by $Q^1 \to Q^0Z^1$ and (ii) Q^1Z^1 production followed by the decays: $Q^1 \to Q'^0W^1$ and Z^1 decay producing two leptons with γ^1 (in two steps). The SM background for the three-lepton plus jet and missing p_T final state will arise from $t\bar{t}$ production, WZ or $W\gamma^*$ production in association with a jet.

The first step in enhancing the signal compared to the background is to apply the jet-lepton isolation cut ($\Delta R > 0.7$) on every lepton. For $R^{-1} = 500$ GeV, the three-lepton background that still survives turns out to be about three times the signal. We order the three leptons in

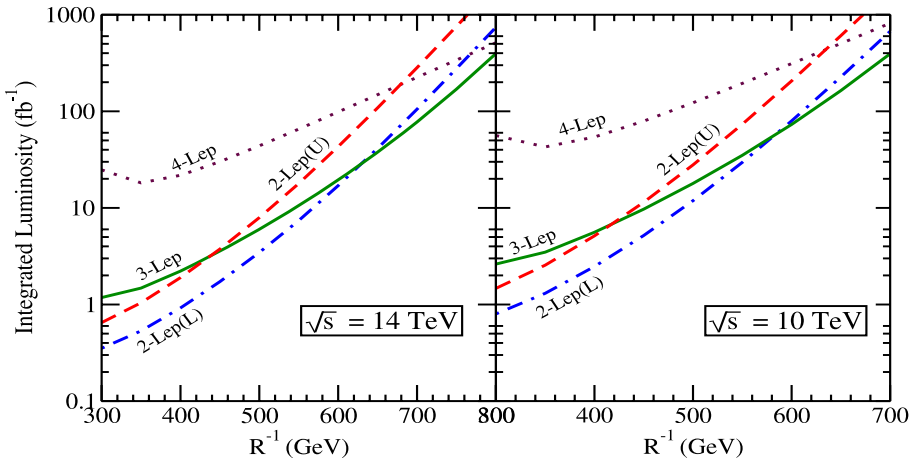

Fig. 3. The required integrated luminosity at the LHC running at $\sqrt{s} = 14$ TeV (left panel) and 10 TeV (right panel) for a 5σ signal in the multilepton + 1 jet + missing p_T channels as a function of R^{-1}. Results are shown for 2-, 3-, and 4-leptons. 'U' and 'L' correspond to the cases of unlike- and like-lepton flavors. (For interpretation of the references to color in this figure legend, the reader is referred to the web version of this article.)

Table 6
Cross section (in fb) at the LHC of signal and background for the trilepton plus one jet and missing p_T channel for $R^{-1} = 500$ GeV.

$\sqrt{s} \rightarrow$	14 TeV		10 TeV	
Cut used ↓	Signal	Background	Signal	Background
Basic cuts	9.39	1183.21	3.21	555.85
Lepton isolation	6.96	21.69	2.41	10.53
${p_T}^{l_2} < 25$ GeV	5.63	4.09	2.01	1.75
${p_T}^{l_3} < 40$ GeV	5.12	1.31	1.86	0.64
$\lvert M_{l_i l_j} - M_Z \rvert > 10$ GeV	5.03	1.16	1.82	0.57

increasing p_T: ${p_T}^{l_1} < {p_T}^{l_2} < {p_T}^{l_3}$ and apply additional cuts to enhance the signal compared to the background.

As for the two-lepton case, here again the p_T of leptons from KK-mode decay are peaked in the lower range with distributions not extending to high values. So, it is useful to demand that the p_T of the leptons be confined to a judiciously chosen window. Further, to remove any Z-related background, one must apply a cut on the invariant mass of all possible pairings of leptons. Thus, we are led to the following kinematic cuts:

(i) ${p_T}^{l_2} < 25$ GeV,
(ii) ${p_T}^{l_3} < 40$ GeV,
(iii) $\lvert M_{l_i l_j} - M_Z \rvert > 10$ GeV for $i, j = 1, 2, 3,\ i \neq j$.

The effect of these successive cuts is readily seen from Table 6. For a 10 fb^{-1} integrated luminosity with LHC running at $\sqrt{s} = 14$ (10) TeV, significance which is initially 0.86 (0.43) achieves a respectable value of 6.39 (3.72) after the kinematic cuts. In Fig. 3 is shown (green solid curve) the integrated luminosity necessary for a 5σ signal as a function of R^{-1}. It is seen that with 100 fb^{-1}

Table 7
Cross section (in fb) at the LHC of signal and background for the tetralepton plus one jet and missing p_T channel for $R^{-1} = 500$ GeV.

$\sqrt{s} \rightarrow$	14 TeV		10 TeV	
Cut used $\downarrow$	Signal	Background	Signal	Background
Basic cuts	1.01	0.130	0.350	0.068
Lepton isolation	0.665	0.029	0.233	0.015
$\lvert M_{l_i l_j} - M_Z \rvert > 10$ GeV	0.573	0.004	0.206	0.002

data one will have a reach in R^{-1} of 720 (620) GeV at the 5σ level through this trilepton mode with the LHC running with $\sqrt{s} = 14$ (10) TeV.

4.5. Four leptons

The signal consisting of four leptons, a jet and missing p_T will arise from $Q^1 Z^1$ production, followed by the Q^1 decaying through a Z^1. The background, in the Standard Model, originates from four W-bosons or three Z-bosons, in either case associated with a jet. These processes are expected to be small. This is borne out by the results presented in Table 7. To enrich the signal with respect to the background all leptons are required to be isolated ($\Delta R > 0.7$) from the jet. Further, to eliminate the background from Z-boson decays we require:

$$|M_{l_i l_j} - M_Z| > 10 \text{ GeV} \quad \text{for } i, j = 1, 2, 3, 4,\ i \neq j.$$

It is seen that the signal and background are both small. The minimum integrated luminosity required for a 5σ discovery as a function of R^{-1} is shown in Fig. 3 (brown dotted curve). With a data set of 100 fb^{-1} the reach of the four-lepton channel is 600 (500) GeV for the LHC running with $\sqrt{s} = 14$ (10) TeV.

5. Conclusions and outlook

Universal extra-dimensional models provide a rich spectrum of towers of KK excitation modes of the SM particles. These KK modes are characterised by the integers $n = 1, 2, 3 \ldots$. They bear the same quantum numbers as their zero-mode counterparts but carry higher masses with constant spacing, given by n/R (upto zero mode masses). Bearing in mind all the different experimental constraints on R, the lowest (i.e., $n = 1$) KK excitations can still be very much within the reach of the LHC. Due to the conservation of KK number at the tree level vertices which follows from the symmetry of the Lagrangian, such KK modes are likely to be produced in pairs. Quantum corrections cause splitting among the different KK states at the same level. The lightest of the $n = 1$ states – the γ^1 – is stable and escapes undetected. In this paper, from the point of view of signal to background optimization (see Introduction), we have focussed on the production of the $n = 1$ excitation of a gauge boson along with an $n = 1$ excited quark.

The decay of the gauge boson excitations gives rise to leptons and missing p_T (from the undetected γ^1) while the quark excitation produces a jet, missing p_T and possibly leptons. Thus, the signal is a jet, several leptons and missing p_T. The SM background for these final state topologies is larger than the signal, sometimes overwhelmingly. We have shown that with judiciously chosen kinematic cuts, including an isolation of the jet from all leptons, the signal can be enhanced *vis-à-vis* the background, while retaining enough signal events for a positive verdict with 100 fb^{-1}

of data. This will be possible so long as R^{-1} does not exceed about 700–800 GeV considering that the LHC would have an accumulated luminosity of (100–300) fb^{-1} at $\sqrt{s} = 14$ TeV.

We have classified the cuts in two categories. First, we imposed some basic cuts to suit LHC observability: (i) the leptons are required to satisfy $p_T > 5$ GeV, (ii) the jet must have a p_T not less than 20 GeV, and (iii) the missing transverse momentum must be more than 25 GeV. Beyond this, other kinematic cuts have been appropriately imposed on a case-by-case basis depending on the number of leptons in the final state. Out of these, two cuts deserve special mention: (i) the requirement of an isolation of the jet from all leptons is found to be quite useful to remove the top and bottom quark related backgrounds, and (ii) a cut on the lepton-pair invariant mass to remove on-shell SM Z production backgrounds is also quite effective. Our main observation for the specific UED signal cross sections at the LHC with $\sqrt{s} = 14$ TeV after the imposition of the kinematic cuts is as follows:

- Single jet $+ \not{p}_T +$ two leptons: Signal:12.52 fb, Background: 9.18 fb,
- Single jet $+ \not{p}_T +$ three leptons: Signal: 5.03 fb, Background: 1.16 fb,
- Single jet $+ \not{p}_T +$ four leptons: Signal: 0.573 fb, Background: 0.004 fb.

The analysis performed here is based on a parton-level simulation and is of an exploratory nature. For example, it has been assumed that the detectors are of perfect efficiency, QCD corrections have not been included, and parton distribution function uncertainties ignored. Our results encourage a detailed careful analysis with full detector simulation.

It should be observed that the spectrum and the couplings in UED or such extra-dimensional models are reminiscent of many different non-supersymmetric scenarios which contain additional gauge bosons and/or vector-like fermions. A crucial component of UED is the presence of a stable γ^1 which makes it different from its peers. The following observation is worth noticing. Conceptually, UED is closer to the Randall–Sundrum (RS) scenario than supersymmetry, so one would naively expect similar observational features between UED and RS than, say, between UED and supersymmetry. First recall the similarities between UED and RS. Although, the extra space is warped for RS and flat for UED, both yield KK modes as a consequence of compactification of an extra space dimension, and in both cases, the SM particles and their KK partners share the same spin. This is in contrast to the supersymmetric extension of the SM (which may be interpreted as a theory with an extra dimension in fermion coordinates), where the SM particles and their superpartners carry different spin. Nonetheless, it turns out that from an observational point of view, UED is closer to supersymmetry with conserved R-parity (or, for that matter, little Higgs models with conserved T-parity) than RS. This happens primarily because the simplest version of RS lacks a stable γ^1 due to the absence of KK parity, while supersymmetry with conserved R-parity (or, little Higgs with conserved T-parity) does contain a stable superparticle (heavy particle). Quite a few LHC simulations of the RS scenario have been carried out [38]. But due to the absence of any KK parity in the simplest versions of RS, the KK states, once produced, decay into the SM particles, and hence the search strategies for RS and UED would be entirely different. However, as already mentioned in the Introduction, weak-scale supersymmetry, with a relatively compressed spectrum, can mimic UED and *vice-versa* at LHC. Distinction between these two new physics alternatives can only be done by exploiting the spin information imprinted in angular distributions. A detailed study of how to differentiate UED from supersymmetry, following our line of analysis in the context of the LHC, is beyond the scope of the present work.

Acknowledgements

G.B. and A.D. are partially supported by project No. 2007/37/9/BRNS (DAE), India. A.D. is also supported in part by CSIR project No. 03(1085)/07/EMR(II) and the UGC DRS programme (F 530/4/DRS/2009 (SAP 1)). The work of S.K.M. is partially supported by the Belgian Federal Office for Scientific, Technical and Cultural Affairs through the Inter-university Attraction Pole No. P6/11. We thank P. de Aquino for cross-checking some of our results using the MG and FR-MUED implementation. S.K.M. is thankful to F. Maltoni for useful discussions. S.K.M. also thanks Saha Institute of Nuclear Physics for hospitality at different stages of the work. The research of A.R. was supported under the XI Plan Neutrino Physics and Regional Centre for Accelerator-based Particle Physics projects at HRI. The initial computational work was carried out using the HRI cluster facilities.

References

[1] N. Arkani-Hamed, S. Dimopoulos, G.R. Dvali, Phys. Lett. B 429 (1998) 263, arXiv:hep-ph/9803315;
I. Antoniadis, N. Arkani-Hamed, S. Dimopoulos, G.R. Dvali, Phys. Lett. B 436 (1998) 257, arXiv:hep-ph/9804398;
N. Arkani-Hamed, S. Dimopoulos, G.R. Dvali, Phys. Rev. D 59 (1999) 086004, arXiv:hep-ph/9807344.
[2] I. Antoniadis, Phys. Lett. B 246 (1990) 377.
[3] E. Accomando, I. Antoniadis, K. Benakli, Nucl. Phys. B 579 (2000) 3, arXiv:hep-ph/9912287.
[4] P. Nath, Y. Yamada, M. Yamaguchi, Phys. Lett. B 466 (1999) 100, arXiv:hep-ph/9905415.
[5] M. Masip, A. Pomarol, Phys. Rev. D 60 (1999) 096005, arXiv:hep-ph/9902467.
[6] T.G. Rizzo, J.D. Wells, Phys. Rev. D 61 (2000) 016007, arXiv:hep-ph/9906234;
A. Strumia, Phys. Lett. B 466 (1999) 107, arXiv:hep-ph/9906266;
C.D. Carone, Phys. Rev. D 61 (2000) 015008, arXiv:hep-ph/9907362.
[7] T. Appelquist, H.C. Cheng, B.A. Dobrescu, Phys. Rev. D 64 (2001) 035002, arXiv:hep-ph/0012100.
[8] P. Dey, G. Bhattacharyya, Phys. Rev. D 70 (2004) 116012, arXiv:hep-ph/0407314;
P. Dey, G. Bhattacharyya, Phys. Rev. D 69 (2004) 076009, arXiv:hep-ph/0309110.
[9] P. Nath, M. Yamaguchi, Phys. Rev. D 60 (1999) 116006, arXiv:hep-ph/9903298.
[10] D. Chakraverty, K. Huitu, A. Kundu, Phys. Lett. B 558 (2003) 173, arXiv:hep-ph/0212047.
[11] A.J. Buras, M. Spranger, A. Weiler, Nucl. Phys. B 660 (2003) 225, arXiv:hep-ph/0212143;
A.J. Buras, A. Poschenrieder, M. Spranger, A. Weiler, Nucl. Phys. B 678 (2004) 455, arXiv:hep-ph/0306158.
[12] K. Agashe, N.G. Deshpande, G.H. Wu, Phys. Lett. B 514 (2001) 309, arXiv:hep-ph/0105084.
[13] J.F. Oliver, J. Papavassiliou, A. Santamaria, Phys. Rev. D 67 (2003) 056002, arXiv:hep-ph/0212391.
[14] T. Appelquist, H.U. Yee, Phys. Rev. D 67 (2003) 055002, arXiv:hep-ph/0211023.
[15] T. Rizzo, Phys. Rev. D 64 (2001) 095010, arXiv:hep-ph/0106336;
C. Macesanu, C.D. McMullen, S. Nandi, Phys. Rev. D 66 (2002) 015009, arXiv:hep-ph/0201300;
C. Macesanu, C.D. McMullen, S. Nandi, Phys. Lett. B 546 (2002) 253, arXiv:hep-ph/0207269;
H.-C. Cheng, Int. J. Mod. Phys. A 18 (2003) 2779, arXiv:hep-ph/0206035;
A. Muck, A. Pilaftsis, R. Rückl, Nucl. Phys. B 687 (2004) 55, arXiv:hep-ph/0312186.
[16] U. Haisch, A. Weiler, Phys. Rev. D 76 (2007) 034014, arXiv:hep-ph/0703064.
[17] G. Servant, T.M.P. Tait, Nucl. Phys. B 650 (2003) 391, arXiv:hep-ph/0206071.
[18] N. Arkani-Hamed, M. Schmaltz, Phys. Rev. D 61 (2000) 033005, arXiv:hep-ph/9903417.
[19] A. Delgado, A. Pomarol, M. Quiros, JHEP 0001 (2000) 030, arXiv:hep-ph/9911252.
[20] N. Arkani-Hamed, H.C. Cheng, B.A. Dobrescu, L.J. Hall, Phys. Rev. D 62 (2000) 096006, arXiv:hep-ph/0006238.
[21] K. Dienes, E. Dudas, T. Gherghetta, Nucl. Phys. B 537 (1999) 47, arXiv:hep-ph/9806292.
[22] K.R. Dienes, E. Dudas, T. Gherghetta, Phys. Lett. B 436 (1998) 55, arXiv:hep-ph/9803466;
For a parallel analysis based on a minimal length scenario, see: S. Hossenfelder, Phys. Rev. D 70 (2004) 105003, arXiv:hep-ph/0405127.
[23] G. Bhattacharyya, A. Datta, S.K. Majee, A. Raychaudhuri, Nucl. Phys. B 760 (2007) 117, arXiv:hep-ph/0608208.
[24] G. Bhattacharyya, S.K. Majee, A. Raychaudhuri, Nucl. Phys. B 793 (2008) 114, arXiv:0705.3103 [hep-ph].
[25] H.C. Cheng, K.T. Matchev, M. Schmaltz, Phys. Rev. D 66 (2002) 036005, arXiv:hep-ph/0204342.
[26] M. Puchwein, Z. Kunszt, Ann. Phys. 311 (2004) 288, arXiv:hep-th/0309069.

[27] H. Georgi, A.K. Grant, G. Hailu, Phys. Lett. B 506 (2001) 207, arXiv:hep-ph/0012379.
[28] G. von Gersdorff, N. Irges, M. Quiros, Nucl. Phys. B 635 (2002) 127, arXiv:hep-th/0204223.
[29] Macesanu, McMullen and Nandi in [15].
[30] Rizzo in [15].
[31] H.C. Cheng, K.T. Matchev, M. Schmaltz, Phys. Rev. D 66 (2002) 056006, arXiv:hep-ph/0205314.
[32] J.M. Smillie, B.R. Webber, JHEP 0510 (2005) 069, arXiv:hep-ph/0507170.
[33] A. Datta, K. Kong, K.T. Matchev, Phys. Rev. D 72 (2005) 096006, arXiv:hep-ph/0509246;
A. Datta, K. Kong, K.T. Matchev, Phys. Rev. D 72 (2005) 119901, Erratum.
[34] G. Bhattacharyya, P. Dey, A. Kundu, A. Raychaudhuri, Phys. Lett. B 628 (2005) 141, arXiv:hep-ph/0502031;
A. Datta, S.K. Rai, Int. J. Mod. Phys. A 23 (2008) 519, arXiv:hep-ph/0509277;
Identifications of $n = 2$ KK gauge modes have also been analyzed, see: B. Bhattacherjee, A. Kundu, S.K. Rai, S. Raychaudhuri, Phys. Rev. D 78 (2008) 115005, arXiv:0805.3619 [hep-ph];
B. Bhattacherjee, A. Kundu, Phys. Lett. B 627 (2005) 137, arXiv:hep-ph/0508170.
[35] J. Pumplin, D.R. Stump, J. Huston, H.L. Lai, P.M. Nadolsky, W.K. Tung, JHEP 0207 (2002) 012, arXiv:hep-ph/0201195.
[36] F. Maltoni, T. Stelzer, JHEP 0302 (2003) 027, arXiv:hep-ph/0208156.
[37] N.D. Christensen, C. Duhr, arXiv:0806.4194 [hep-ph].
[38] K. Agashe, S. Gopalakrishna, T. Han, G.Y. Huang, A. Soni, arXiv:0810.1497 [hep-ph];
K. Agashe, et al., Phys. Rev. D 76 (2007) 115015, arXiv:0709.0007 [hep-ph];
K. Agashe, A. Belyaev, T. Krupovnickas, G. Perez, J. Virzi, Phys. Rev. D 77 (2008) 015003, arXiv:hep-ph/0612015;
K. Agashe, G. Perez, A. Soni, Phys. Rev. D 75 (2007) 015002;
F. Ledroit, G. Moreau, J. Morel, JHEP 0709 (2007) 071, arXiv:hep-ph/0703262;
A. Djouadi, G. Moreau, R.K. Singh, Nucl. Phys. B 797 (2008) 1, arXiv:0706.4191 [hep-ph].